# Effects of the Earth Orbit Environment on Thin-Wall Bubbles

Scott Thomas*
*Utah State University, Logan, Utah 84322*

**The use of thin-wall bubbles and erectable films has been proposed for a variety of applications in Earth orbit. These structures would be blown or erected from curable liquids. In this paper, the effects of the space environment on such structures are analyzed. Effects due to thermal loads, high vacuum, ram pressure, and atomic oxygen ablation are considered. The low thermal mass and large area of the structures lead to a strong coupling with the thermal environment. Large temperature gradients and swings (~100 K) can be expected. Although potentially detrimental, these properties could be advantageous to satellite thermal control systems. For liquid structures, the relatively low vacuum leads to very long mechanical damping times (hours). A finite liquid vapor pressure can also render closed structures unstable to bursting. The proposed structures have a very small mass per surface area giving a large ballistic coefficient. Atmospheric drag is therefore significant. Liquid structures can deform or collapse. The orbital lifetime of a free bubble can be very short (fractions of an orbit) and sensitive to the ambient density. This sensitivity could prove to be a useful tool to study atmospheric density at orbital altitudes. Associated with the drag process is the problem of atomic oxygen ablation at orbital velocities. The thin nature of the structures can lead to short disintegration times (hours) by ablation.**

## Nomenclature

$A$ = bubble surface area
$A_\perp$ = cross-sectional area
$a$ = absorptivity at optical wavelengths
$a_v$ = acceleration due to viscous force
$\boldsymbol{B}$ = magnetic field
$C_D$ = drag coefficient
$c_w$ = specific heat of bubble wall
$E_T$ = thermal energy of bubble
$F$ = drag force
$F_v$ = viscous force in bubble wall
$F(\xi)$ = force on disturbance $\xi$
$f_c$ = collision parameter
$G$ = gravitational constant
$H_{\text{bub}}$ = radiant intensity inside bubble
$H_{\text{ext}}$ = external radiant intensity
$H_{\text{loss}}$ = emitted radiant intensity
$H_0$ = normal external radiant intensity
$K$ = ablation rate
$L$ = radius of bubble blower
$M$ = mass of Earth
M = molecular weight of bubble wall
$m$ = mass of bubble
$N_A$ = Avogadro's number
$\boldsymbol{n}$ = unit inward normal
$n$ = ambient number density
$P$ = radiant power
$P_g$ = partial pressure of insoluble gas
$P_i$ = pressure inside bubble
$P_s$ = partial pressure of soluble gas
$P_v$ = liquid vapor pressure
$\nabla P$ = pressure gradient in bubble wall
$P_0$ = ambient pressure
$\boldsymbol{R}$ = distance from center of Earth
$r$ = bubble radius
$r_1$ = radius of inner bubble surface
$r_2$ = radius of outer bubble surface
$r_0$ = equilibrium bubble radius
$s$ = arc length
$T$ = temperature
$T_b$ = temperature at back of bubble
$T_f$ = temperature at front of bubble
$U$ = potential energy of disturbance
$u$ = velocity in bubble wall
$V$ = bubble volume
$\mathbf{v}$ = orbital velocity
$\boldsymbol{x}$ = coordinates of point on bubble surface
$x$ = distance from center along symmetry axis
$y$ = distance from symmetry axis
$\alpha$ = angle between velocity vector and surface normal
$\beta$ = ballistic coefficient
$\Gamma$ = amplification factor for disturbances
$\gamma$ = inverse time constant for damping
$\delta$ = bubble wall thickness
$\epsilon$ = emissivity at infrared wavelengths
$\epsilon_{\text{eff}}$ = ablation efficiency
$\eta$ = absolute viscosity of liquid
$\theta$ = polar coordinate
$\lambda$ = angle between surface tangent and symmetry axis
$\mu$ = deformation parameter
$\nu$ = kinematic viscosity of liquid
$\xi$ = magnitude of spherical disturbance
$\rho$ = ambient mass density
$\rho_w$ = mass density of bubble wall
$\sigma$ = surface tension
$\partial\sigma/\partial T$ = surface tension coefficient with temperature
$\sigma_{\text{SB}}$ = Stefan-Boltzmann constant
$\tau_d$ = disintegration time constant
$\tau_T$ = thermal time constant
$\tau_v$ = viscous damping time constant
$\omega_0$ = natural frequency of bubble

## Introduction

THE purpose of this paper is to characterize the effects of the near-Earth space environment on large, thin-wall bubbles and films. A thin-wall bubble is defined here as a thin (1–100 $\mu$m) shell of solid or liquid surrounding a low-density gas. A bubble or film, blown, erected, or released into Earth orbit can be significantly affected by environmental factors such as the high vacuum, thermal loads, ram pressure, and atomic oxygen ablation by the ambient atmosphere. This work

Received May 17, 1989; revision received Jan. 6, 1990. 

*Research Assistant, Center for Atmospheric and Space Sciences.

was undertaken in order to identify and to quantify these effects in relation to their impact on possible practical applications. Emphasis has been placed on size and lifetime limits and altitude dependence. Thin-wall bubbles or erectable films may have a number of applications in low Earth orbit.[1] These include optical mirrors, radio frequency antennas, solar collectors, thermal radiators, wake shields, and, as will be shown, scientific probes of the mass density and ablative properties of the ambient atmosphere. Some of these applications could be filled by conventional inflatables, but bubbles, being thinner, have the advantage of requiring less raw material and can be formed in situ.[1]

A bubble would be formed by creating a thin liquid film and then "blowing" a gas on one side of the film. If liquid can be added to the film, in principle, because of the lack of gravity, the bubble can be "blown" indeterminately large. As will be shown in the following, though, there are a number of environmental factors that limit the maximum achievable size. Depending on the application, the bubble could stay attached to, or be released from, the blowing mechanism. In addition, rigid or erectable frames could be used to define the shape of the bubble or form thin films. After the desired configuration is achieved, the liquid film could be solidified by photo polymerization, thermal setting, binary curing, etc.

The use of bubbles in low Earth orbit requires a knowledge of the environmental effects and responses. Some applications such as thermal radiators, wake shields, and scientific probes depend on the coupling of the bubble to the environment. It will be shown that the environment puts constraints on the type of materials that can be used, on the usable size, and the lifetime. An understanding of these limits and constraints is needed to assess which applications are practical. Undesirable responses to the environment may also be overcome if they are sufficiently understood.

## Analysis of Environmental Effects

As stated above, a thin wall bubble is defined as a thin shell (of solid or liquid) surrounding a low density gas. At the ambient pressures in Earth orbit, the mass of the enclosed gas is negligible compared to the mass in the wall (although this is not the case at atmospheric pressures). The mass of the bubble is therefore taken to be

$$m = 4\pi r^2 \delta \rho_w \tag{1}$$

The total mass is very small, e.g., a 1-m-diam bubble with a 1-$\mu$m wall has a mass of only 3–4 g. Since the total mass is small, the total specific heat is small and resides in the wall. Owing to the small inertial and thermal mass, the bubble is very gossamer mechanically and thermally. This is the crux of many of the applications stated above but is also why environmental factors, usually not significant, are so important.

The pressure drop across the surface of a liquid wall bubble is given by the Young-Laplace equation. For spherical symmetry

$$P_i - P_0 = \frac{4\sigma}{r_0} \tag{2}$$

The $P_0$ can be on the order of $4\sigma/r_o$, so pressure terms such as the ram pressure or liquid vapor pressure can have large effects on shape and stability. These are not applicable to solid-wall bubbles, but presumably the solid wall was formed from a liquid phase; these effects must therefore be considered.

We will discuss the effects of the thermal environment, the relatively high vacuum, and the ambient atmosphere. The high vacuum effects and deformation due to ram pressure are applicable only to liquid wall bubbles. The other effects are important for liquid or solid wall bubbles. The effects of the plasma environment and $\mathbf{v} \times \boldsymbol{B}$ field are not described. Except for the case where a bubble is intentionally charged to many thousands of volts, these effects are insignificant compared to the effects detailed below.

### Thermal

A bubble in Earth orbit will be radiatively coupled to the environment. The radiant intensity from the sun is about 1350 W/m$^2$, and in low Earth orbit about 240 W/m$^2$ from the Earth. The thermal power radiated away by the bubble is

$$P = \epsilon \sigma_{SB} A T^4 \tag{3}$$

The total thermal energy of the bubble is the heat capacitance times temperature.

$$E_T = \rho_w c_w \delta A T \tag{4}$$

When a bubble crosses the terminator between day and night, the input radiant flux changes by a factor of over 5. The equilibrium temperature changes with a time constant on the order of the total energy divided by the power radiated away

$$\tau_T \sim \frac{\rho_w c_w \delta}{\epsilon \sigma_{SB} T^3} \tag{5}$$

Note that this is independent of bubble size. For a 1-$\mu$m wall bubble at $T = 300$ K with $\epsilon = 1$, we find $\tau \sim 3$ s. A bubble is, therefore, strongly coupled to the thermal environment owing to its small mass and large area.

To find the equilibrium temperature profile, we must consider thermal transport within the bubble. Conduction and convection are insignificant in the wall due to its small thickness, and so we consider only radiative transport. Since essentially all of the thermal mass resides in the wall, our model will be a spherical shell with an external radiant intensity incident from one direction. The temperature profile (on the shell) is assumed axially symmetric about the direction of the incident radiation ($\theta = 0$). The shell is assumed partially opaque at infrared wavelengths with emissivity $\epsilon$ (equal to the infrared absorptivity) and either opaque or nearly transparent at optical wavelengths with absorptivity $a$. In equilibrium, the total flux over every element of area on the shell must be zero. The contributions to the total are the external flux, the loss radiated inward and outward, and the flux from the rest of the shell. The flux balance is

$$(H_{ext} - H_{loss} + H_{bub})\, dA = 0 \tag{6a}$$

for every element $dA$. Dividing out $dA$ and giving the explicit expressions for $H$,

$$aH_0 |\cos\theta| - 2\epsilon\sigma_{SB} T^4(\theta) + \int_{shell} dH' = 0 \tag{6b}$$

everywhere on the shell, where $\theta$ is the angle between the outward normal of the shell and the incident flux. The infinitesimal intensity $dH'$, at position $\boldsymbol{x}$, from an element of area at $\boldsymbol{x}'$, can be written[2]

$$dH' = \frac{\epsilon\sigma_{SB} T^4}{\pi} \left\{ \frac{\boldsymbol{n}\cdot(\boldsymbol{x}-\boldsymbol{x}')\, \boldsymbol{n}'\cdot(\boldsymbol{x}-\boldsymbol{x}')}{|\boldsymbol{x}-\boldsymbol{x}'|^4} \right\} dA' \tag{7a}$$

where $\boldsymbol{n}$, $\boldsymbol{n}'$ are the inward normals of the shell at $\boldsymbol{x}$, $\boldsymbol{x}'$. Equation (7a) neglects internal reflections. This is a good approximation at infrared wavelengths where most of the unabsorbed radiation may pass through the thin film. For a spherical shell, the term in brackets is equal to $(4r)^{-2}$ for any

$(x, x')$ pair. Equation (6b) then becomes

$$aH_0 |\cos\theta| - 2\epsilon\sigma_{SB}T^4(\theta) + \frac{\epsilon\sigma_{SB}}{2}\int_0^\pi T^4(\theta')\sin\theta' d\theta' = 0 \qquad (7b)$$

For an optically opaque bubble, the external flux term is zero on the back half of the shell, and so $T$ is constant over $\pi/2 < \theta < \pi$. For a nearly optically transparent bubble, the external flux is nearly the same on the front and back half, so we take $T$ to be symmetric about $\theta = \pi/2$ in this case. For either case we see from Eq. (7b) that

$$T^4\left(\frac{\pi}{2}\right) = \frac{1}{4}\int_0^\pi T^4(\theta')\sin\theta' d\theta' \qquad (8a)$$

and so the solution is of the form

$$T^4(\theta) = T^4\left(\frac{\pi}{2}\right) + \frac{aH_0|\cos\theta|}{2\epsilon\sigma_{SB}} \qquad (8b)$$

Substituting Eq. (8b) into (7b) we find for a free bubble

$$T^4(\theta) = \frac{aH_0}{2\epsilon\sigma_{SB}}\left(\frac{1}{4} + \cos\theta\right) \qquad 0 \le \theta \le \frac{\pi}{2} \text{ opaque} \qquad (9a)$$

$$T^4(\theta) = \frac{aH_0}{2\epsilon\sigma_{SB}}\left(\frac{1}{2} + |\cos\theta|\right) \qquad 0 \le \theta \le \pi \text{ transparent} \qquad (9b)$$

The temperature profiles for radiant input from the sun or Earth are given in Fig. 1. Temperature differences across the bubble on the order of 100 K are possible. Temperature swings at the terminator on the order of 100 K are also possible and will take place in only seconds by Eq. (5). Note that the temperature profile is independent of size. The discontinuous gradients at $\theta = \pi/2$ would of course be smeared out by conduction.

If a satellite or blowing mechanism is attached to the bubble, it can act as a net source or sink of heat. If we assume the satellite is at some given temperature and is attached at a point $\theta$, then the temperature profile of the bubble is given by Eq. (8b). Considering only attach points on the back half ($\pi/2 < \theta < \pi$) or front ($\theta = 0$) of an opaque bubble

$$T^4(\theta) = T_b^4 + \frac{aH_0}{2\epsilon\sigma_{SB}}\cos\theta \qquad (T_b \text{ specified}) \qquad (10a)$$

$$T^4(\theta) = T_f^4 + \frac{aH_0}{2\epsilon\sigma_{SB}}(\cos\theta - 1) \qquad (T_f \text{ specified}) \qquad (10b)$$

where $T_b$ or $T_f$ is the source (or sink) temperature on the front or back bubble surface respectively. The net power sourced or sinked by the satellite is the power radiated away minus the total incident power. Using the temperature distributions of Eqs. (10) and assuming radiative loss over $4\pi$ steradians,

$$P_{net} = A\left(\epsilon\sigma_{SB}T_b^4 - \tfrac{1}{8}aH_0\right) \qquad (T_b \text{ specified}) \qquad (11a)$$

$$P_{net} = A\left(\epsilon\sigma_{SB}T_f^4 - \tfrac{5}{8}aH_0\right) \qquad (T_b \text{ specified}) \qquad (11b)$$

The power per unit bubble surface area sourced by an attached satellite at a temperature $T$ is plotted in Fig. 2. The total power sourced or sinked is quite large for $T_b$ or $T_f$, significantly different from the equilibrium temperature of a free bubble. If power cannot be sourced (or sinked) by the satellite, it will, of course, eventually reach the equilibrium temperature of a free bubble – the time constant for which is determined only by how fast thermal energy can be transferred within the satellite.

The large temperature gradients and swings can have a number of severe effects. These include deformation or rupture of the wall during a temperature swing or nonuniform curing along the bubble. In a liquid wall bubble, thermocapillary flow will occur since the surface tension of a liquid depends on temperature. The thermally induced surface tension gradient is balanced by shear stress in the film, and a pressure gradient and small flow result.[3] The pressure gradient will cause liquid in the wall to "drain" toward a lower temperature, much as the hydrostatic pressure gradient causes a bubble wall to drain downward in the terrestrial environment.[4] The magnitude of the thermocapillary pressure gradient is[3]

$$\nabla P \sim \frac{(\partial\sigma/\partial T)\nabla T}{\delta} \qquad (12)$$

For a typical set of values ($\delta = 1$ μm, $\partial\sigma/\partial T = 0.1$ dyne/cm, $\nabla T = 1$ K/cm), the pressure gradient, and therefore the draining rate, is the same order as the hydrostatic gradient that would result in the terrestrial environment.

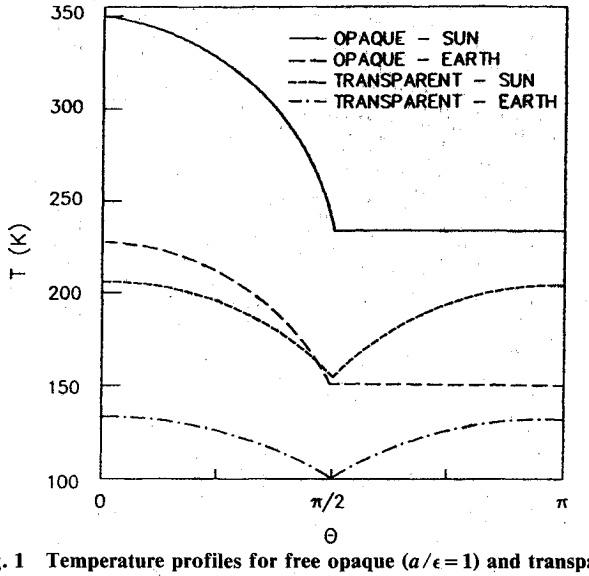


**Fig. 1 Temperature profiles for free opaque ($a/\epsilon = 1$) and transparent ($a/\epsilon = 0.1$) bubbles with radiative input from the sun ($H_0 = 1350$ W/m²) or Earth (240 W/m²).**

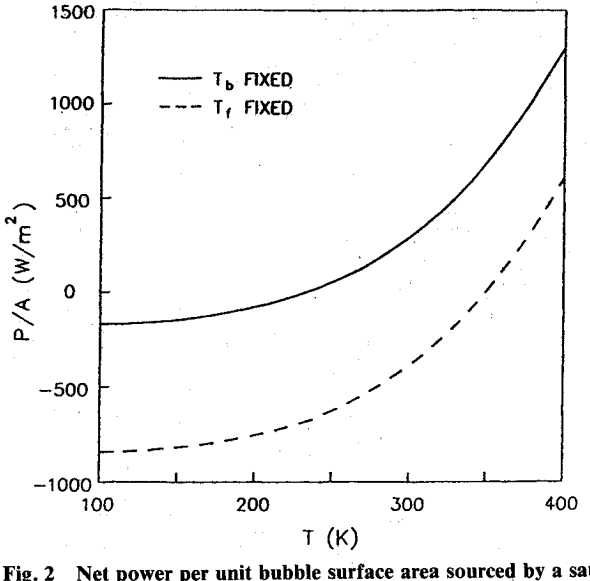


**Fig. 2 Net power per unit bubble surface area sourced by a satellite of temperature $T$ attached to the back half or front of a bubble; $a/\epsilon = 1$, $H_0 = 1350$ W/m².**

**Vacuum**

The pressure environment in low Earth orbit can be very dynamic and complex. For example, at an altitude of 320 km, the ram pressure due to collisions with the ambient atmosphere can be $10^{-5}$ Torr on a frontal surface and drop by two orders of magnitude on a rear surface. The pressure near a spacecraft due to outgassing or thruster firings can be as high as $10^{-4}$ Torr and drop to $10^{-7}$ Torr in the wake.[5] In such relatively low pressures, the only damping of disturbances in the liquid bubble shape will be by viscosity in the wall. It is also well known that bubbles can become unstable (nucleate) when the liquid vapor pressure is on the order of the ambient pressure.[6] We will therefore consider the dynamics and stability of a liquid wall bubble with finite vapor pressure.

We use the simple model of a spherical bubble in a uniform ambient pressure and consider the equation of motion for spherically symmetric disturbances of the surface. The gas inside the bubble is taken to be of three components: 1) a component which does not diffuse through the bubble wall and satisfies the ideal gas law, 2) a component which is produced at a uniform rate inside the bubble and is entirely soluble in the bubble wall (collides only once with the wall and then diffuses through), and 3) a component caused by the outgassing of the liquid. The equations of state for the three components are

$$\frac{P_g V}{T} = \text{const} \tag{13a}$$

$$P_s A = \text{const} \tag{13b}$$

$$P_v = \text{const} \tag{13c}$$

The equilibrium of the bubble is given by Eq. (2) with $P_i = P_g + P_s + P_v$.

The potential for a disturbance is just the energy required to create the disturbance.

$$U = \int \sigma \, dA - \int (P_i - P_0) \, dV \tag{14}$$

For an isothermal change in $r$ from the equilibrium $r_0$

$$U(r) = 8\pi\sigma(r^2 - r_0^2) - 4\pi(P_0 - P_v - P_s) r_0^3 \, \ell n\left(\frac{r}{r_0}\right) - 16\pi\sigma r_0^2 \, \ell n\left(\frac{r}{r_0}\right) + \frac{4}{3}\pi(P_0 - P_v)(r^3 - r_0^3) - 4\pi P_s r_0^2 (r - r_0) \tag{15}$$

where we have used Eq. (2) to eliminate $P_g$. The force acting on a disturbance, $\xi = r - r_0$, is just $-\nabla U(\xi)$. To lowest order in $\xi$

$$F(\xi) = -[32\pi\sigma + 4\pi r_0(3P_0 - 3P_v - P_s)]\xi \tag{16}$$

The damping for small disturbances is derived in the Appendix; the result is that the damping is proportional to $\dot{\xi}$. The equation of motion for small $\xi$ is, therefore, that of a damped harmonic oscillator

$$\ddot{\xi} + 2\gamma\dot{\xi} + \omega_0^2 \xi = 0 \tag{17a}$$

with

$$\gamma = \frac{3\nu}{r_0^2} \tag{17b}$$

$$\omega_0^2 = \frac{8\sigma}{\rho\delta r_0^2} + \frac{3(P_0 - P_v) - P_s}{\rho\delta r_0} \tag{17c}$$

where we have used Eq. (l) for the mass of the bubble. The frequency of oscillation ($f_0 = \omega_0/2\pi$) is plotted in Fig. 3 as a function of pressure for different radii with $\delta = 1$ $\mu$m.

For ambient pressures much lower than $(4\sigma/r_0)$, the surface tension terms dominate the energy function, and the frequency becomes constant. Conversely, for larger pressures the pressure terms dominate and the frequency varies like the square root of pressure. This increase continues only as long as Eq. (1) is a good approximation. For most applications in Earth orbit, it is expected that surface tension will dominate the oscillations. This is because $P_0$ should be interpreted as the lowest external pressure around the bubble and can be very low for the wakeside of a bubble in the freestream.

The first important result is the damping of disturbances. It is not hard to show that except for the special case $\omega_0^2 \to 0$, discussed below, the motion is highly underdamped. The time constant for disturbances to damp out is then $\gamma^{-1}$.

$$\tau_v = \frac{r_0^2}{3\nu} \tag{18}$$

For a typical viscosity of perhaps 1 Stoke, the time constant for $r_0 = 1$ m is almost 1 h. The other important parameter to consider is the amplification of external perturbations at the natural frequency. The amplification factor for a weakly damped oscillator is $\Gamma = \omega_0/(2\gamma)$. For Eq. (17) with $P_v = P_s = 0$, this becomes

$$\Gamma = \frac{r_0}{\nu}\sqrt{\frac{2\sigma}{9\rho\delta}\left(1 + \frac{3P_0 r_0}{8\sigma}\right)} \tag{19}$$

Even for surface tension dominated oscillations with typical parameters of, $r_0 = 1$ m, $\nu = 1$ cm$^2$/s, $\sigma = 15$ dyne/cm, $\delta = 1$ $\mu$m, $\rho = 1$ g/cm$^3$, we find $\Gamma \sim 10^4 - 10^5$. For amplification factors this large, the entire energy function of Eq. (15) should be used but the order of magnitude would probably not be changed.

The combination of long damping times and large amplification of disturbances near the natural frequency would seem to make the bubble uncontrollable. Any finite disturbance has the potential to amplify to a magnitude large enough to cause the bubble to collapse on itself or to burst due to thinning of

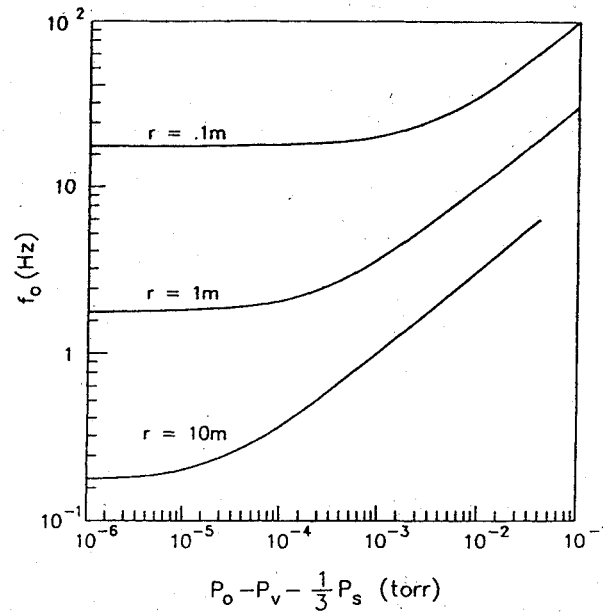


**Fig. 3 Resonant frequency ($f_0 = \omega_0/2\pi$) of spherical oscillations as a function of pressure; $\sigma = 15$ dyne/cm, $\delta = 1$ $\mu$m.**

the wall. Since the damping time is so long compared to the time scale of possible external perturbations from, for example, small lateral motions or rotations, the bubble is effectively never in its equilibrium of stationary spherical symmetry.

One possibility to overcome the detrimental effects of weak damping is to engineer a liquid wall with extremely large viscosity by, for example, using thin film effects, which can increase the effective viscosity by orders of magnitude[7] (at least in the $\omega_0 \to 0$ limit) or by using non-Newtonian shear-thickening liquids. Another possibility would be to use extra supports or struts in the liquid wall thereby reducing the effective $r_0$ in Eqs. (18) and (19) and increasing the effective frequency.

The second important result is that the bubble becomes unstable to small disturbances for large enough $P_v$ and $r_0$. From Eq. (16) the term in brackets is the spring constant for the system. When this becomes negative, small disturbances grow, and the system is unstable. This can also be seen from Eq. (17c) as the condition for imaginary frequencies. Higher-order terms in Eq. (16) show that only $\xi > 0$ disturbances are unstable. The instability will therefore occur as an unbounded growth in $r$ until the bubble wall thins sufficiently to rupture. Physically, the instability occurs when the work done by an expansion of the gas $P\mathrm{d}V$ beomes greater than the energy needed to create new liquid surface $\sigma \mathrm{d}A$. The condition for stability is

$$P_v + \tfrac{1}{3}P_s < (8\sigma/3r_0) + P_0 \tag{20}$$

Equation (20) is plotted in Fig. 4 for different $r_0$. The region of stability is below each curve. Note that for any finite $P_v$ there is some $P_0$ and $r_0$ for which stability is lost, larger $r_0$ being more unstable. For $P_v + 1/3\, P_s < P_0$, stability is guaranteed. When the pressure drop across the bubble is larger than $P_0$ (oscillations are surface tension dominated), instability is possible. Higher modes are volume conserving to lowest order and therefore unimportant in the instability.

In order to find the actual time dependence of the unstable growth, the full energy function of Eq. (15) must be used. However, the time constant for small disturbances to grow can be estimated by solving the equation of motion for Eq. (15) at the point of instability. Expanding in powers of $\xi/r_0$, Eq. (15) with $P_s = 0$ becomes

$$U(\xi) = -\frac{16}{3}\pi\sigma r_0^2 \left\{ \left[\frac{\xi}{r_0}\right]^3 + \sum_{n=4}^{\infty} \frac{(-1)^{n+1}}{n} \left[\frac{\xi}{r_0}\right]^n \right\} \tag{21}$$

when the condition of Eq. (20) is satisfied as an equality. To lowest order, the time for an initial disturbance $\xi_0$ to grow to $O(r_0)$ is then

$$t \cong \frac{(2\sqrt{3})}{\sqrt{\xi_0/r_0}} \sqrt{\frac{\rho \delta r_0^2}{8\sigma}} \tag{22}$$

The term under the last radical sign is just the inverse frequency of a surface tension oscillation. Since the rms $\xi_0$ may be a large fraction of $r_0$, the time constant is therefore just some factor times the inverse natural frequency that would result if the pressure terms were unimportant. This time is long enough to justify the equations of state [Eqs. (13b) and (13c)].

For a bubble attached to a blowing mechanism, the condition for stability is somewhat different. In this case $r_0$ corresponds to the radius of curvature of the liquid film. For a bubble blown from a circular orifice, the radius of curvature is initially infinite when the film is flat. As the bubble is blown, the radius of curvature decreases until it is a hemisphere when the radius of curvature equals the radius of the orifice. As the bubble continues to grow, the radius of curvature again increases. Since the maximum $r_0$ equals the radius

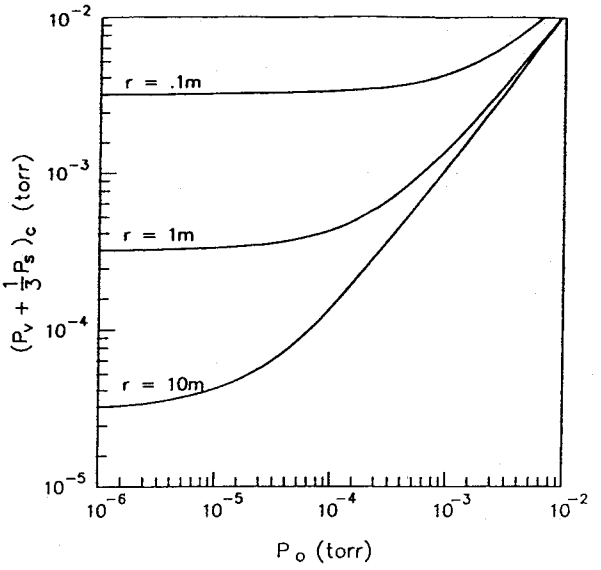


**Fig. 4 Critical vapor pressure for instability as a function of ambient pressure; $\sigma = 15$ dyne/cm.**

of the blower, $L$, the necessary condition for some stable size to exist becomes

$$P_v + \frac{1}{3}P_s < \frac{8\sigma}{3L} + P_0 \tag{23}$$

Figure 4 can also now be interpreted as the maximum orifice size for some equilibrium to exist. The condition of Eq. (23) does not guarantee that a stable bubble can be formed from a flat film since, in general, the flat film is unstable to growing modes if $P_v$ or $P_s$ is finite.

The vapor pressure problem could be greatly reduced by making the blowing chamber and/or bubble partially open to the ambient $P_0$. This would decrease the effective $P_v$ but not eliminate it since the mean free path can be of the order of the bubble size. For $P_v > P_0$ it would be necessary to keep these openings at pressures less than $P_0$ to decrease the destabilizing effects. Also, the use of a Maxwell viscoelastic liquid would add a positive term to the energy function thereby increasing the critical vapor pressure.

### Ram Pressure

The ambient number density in low Earth orbit can be as high as $10^9$ cm$^{-3}$. The mean free path in low Earth orbit is on the order of 1 km. In addition, the average thermal speed is lower than the orbital speed by a factor of about 10. The pressure on a rear-facing surface is therefore down by an order of $10^{-2}$. We will, therefore, assume $P_0 = 0$ on rear surfaces and ballistic collisions on frontal surfaces. With an orbital velocity of the order of 8 km/s, the ram pressure due to collisions can be as high as $10^{-5}$ Torr as stated above. Due to a bubble's small mass and large surface area, the ram pressure can have a number of important effects. For a liquid wall bubble these include the tendency to become dislodged from its blower and to undergo large deformations for $P_{\mathrm{ram}} \sim 4\sigma/r$. The large ballistic coefficient of a free bubble also implies that the re-entry time is very short.

The total force on an object due to the ram pressure is

$$F = C_D f_c \tfrac{1}{2}\rho v^2 A_\perp \tag{24}$$

where $f_c = 1$ for inelastic collisions, and $f_c = 2$ for elastic collisions. The maximum force of adhesion of a liquid bubble to a blower is on the order of twice the surface tension times the circumference of the blower. In order that the bubble stay attached to the blower, this must be greater than the ram

force. For a sphere suffering elastic collisions, this corresponds to

$$r < 8\frac{\sigma}{\rho v^2}\left(\frac{L}{r}\right) \tag{25}$$

Equation (25) is plotted in Fig. 5 for $L/r = 0.1$. The maximum size of an attached liquid bubble is fairly restricted in very low orbit. For some applications it may be necessary to attach extra supports to the bubble in order to increase adhesion or to form it in the wake of another object. Once the bubble is solidified, this is not a restriction.

Next we consider the deformation of a liquid wall bubble caused by the ram pressure. The normal pressure on the front surface is

$$P_0 = f_c \tfrac{1}{2}\rho v^2 \cos^2\alpha \tag{26}$$

The equilibrium shape of a liquid surface is given by the Young-Laplace equation. If we assume axial symmetry about the direction of the velocity vector, the Young-Laplace equation can be written[8]

$$2\sigma\left\{-\frac{y'}{[1+(y')^2]^{3/2}}+\frac{1}{y[1+(y')^2]^{1/2}}\right\} = P_i - P_0 \tag{27}$$

where $' = d/dx$. The term in brackets is twice the mean curvature of an axially symmetric surface described by $y = y(x)$ with $y = 0$ being the symmetry axis. The back half of the bubble is spherical since $P_0 = 0$ and therefore $P_i = 4\sigma/r$. Substituting this and Eq. (26) into Eq. (27) with $f_c = 2$, we get the nondimensional differential equation for the front surface.

$$\frac{y''}{[1+(y')^2]^{-3/2}} = -2+\frac{1}{y[1+(y')^2]^{1/2}}+\frac{2\mu(y')^2}{[1+(y')^2]} \tag{28a}$$

where

$$\mu = \frac{\rho v^2}{4\sigma/r} \tag{28b}$$

The parameter $\mu$ is a ratio of the pressures and sets the scale of the deformation. The coordinate transformation

$$\frac{dx}{ds} = \cos\lambda \qquad \frac{dy}{ds} = \sin\lambda \tag{29}$$

where $ds$ is the differential arc length, brings Eq. (28) into the somewhat more manageable form

$$\frac{d\lambda}{ds} = -2 + |\cos\lambda|\left[\int_0^s \sin\lambda\, ds + y_0\right]^{-1} - 2\mu\sin^2\lambda \tag{30}$$

This also guarantees that the solutions are functions, $\lambda = \lambda(s)$. Equation (30) was integrated numerically using an explicit second order Euler differencing, with initial conditions $\lambda = 0$, $d\lambda/ds = -1$, corresponding to $x = 0$, $y = r_0$, $y' = 0$. The solution was then mapped to the $(x,y)$ plane. The results for different $\mu$ are shown in Fig. 6. The bubble collapses on itself for $\mu = 2.74$. This defines a maximum size for a liquid wall bubble and is plotted in Fig. 5 as a function of altitude. This limit is not too restrictive except at low altitudes.

Finally, we consider the re-entry of a free bubble due to the net drag caused by the ram pressure. The drag acceleration due to the ram pressure is

$$F/m = -C_D\beta f_c \tfrac{1}{2}\rho v^2 \tag{31}$$

where the ballistic coefficient is given by

$$\beta \equiv \frac{A}{m} = \frac{1}{4\rho_w\delta} \tag{32}$$

Note that $\beta$ is independent of $r$ since $m \propto r^2$. The ballistic coefficient for a thin-wall free bubble is very large, and so the re-entry time is very short. In fact, the time is so short that the usual approximations of circular or elliptic orbits with slowly changing radii are not good. To find the trajectory and lifetime, we therefore directly integrate the orbital equations of motion with drag.

$$\ddot{\boldsymbol{R}} = -\frac{GM}{R^3}\boldsymbol{R} + \frac{\boldsymbol{F}}{m} \tag{33}$$

In polar coordinates these become

$$\ddot{R} - R\dot{\theta}^2 = -\frac{GM}{R^2} - C_D\beta\frac{f_c}{2}\rho(R)\left(\dot{R}^2+R^2\dot{\theta}^2\right)\frac{\dot{R}}{\sqrt{\dot{R}^2+R^2\dot{\theta}^2}}$$

$$2\dot{R}\dot{\theta} + R\ddot{\theta} = -C_D\beta\frac{f_c}{2}\rho(R)\left(\dot{R}^2+R^2\dot{\theta}^2\right)\frac{R\dot{\theta}}{\sqrt{\dot{R}^2+R^2\dot{\theta}^2}} \tag{34}$$

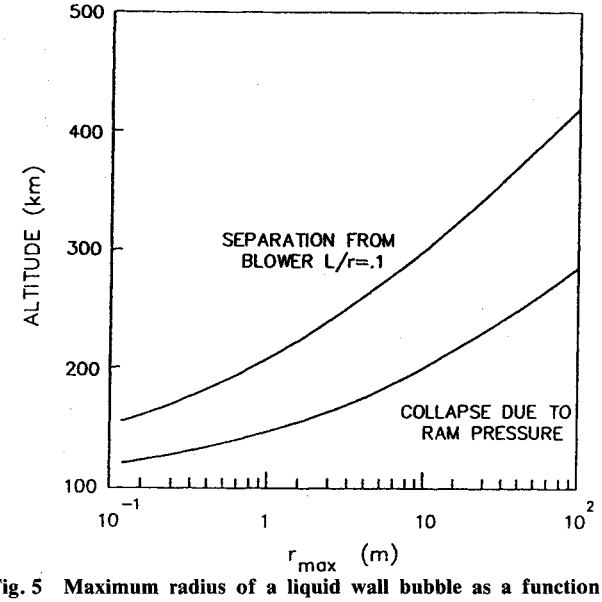


**Fig. 5 Maximum radius of a liquid wall bubble as a function of altitude; $\sigma = 15$ dyne/cm.**

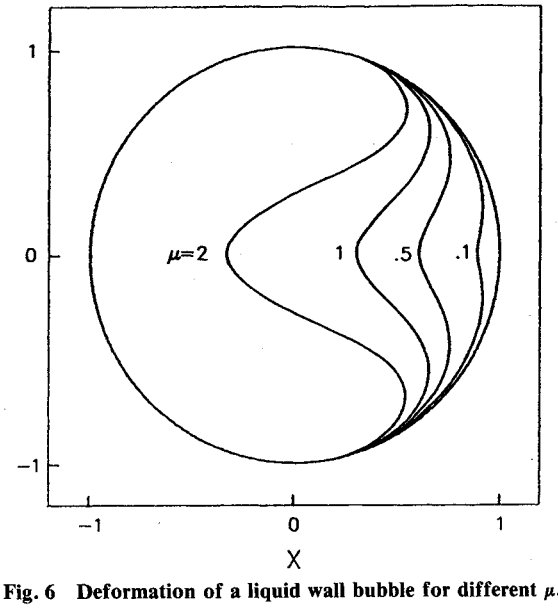


**Fig. 6 Deformation of a liquid wall bubble for different $\mu$.**

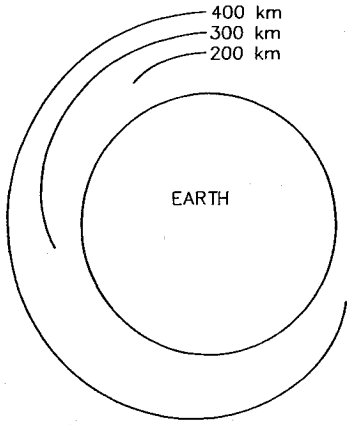


**Fig. 7 Trajectories down to 150 km of spherical bubbles released from circular orbits; $\delta = 1$ μm; the altitude scale outside the Earth is expanded 10 times for clarity.**

Equations (34) were integrated numerically using a second order Euler finite differencing. The time step used was on the order of $10^{-1}$ s, and the accuracy in $R$ per orbit for circular or elliptic orbits with no drag was better than 1 cm. The ambient density profile used was taken from Ref. 9. A value of $f_c = 1.54$ was required to fit the known trajectory of the global low orbiting message relay (GLOMR) satellite launched from the Space Shuttle.[10]

The trajectory for a spherical bubble of 1-μm wall thickness released from a number of circular orbits is shown in Fig. 7. The re-entry time for spherical bubbles of 1- and 10-μm wall thickness, released from initially circular orbits, is given in Fig. 8. Because of the enormous ballistic coefficient, applications of a free bubble must be limited to short durations. This suggests using free bubbles as probes of the ambient density. If the trajectory could be accurately recorded from the ground, the density along the trajectory could be extracted. Actually, the trajectory differs so much from the drag free orbit that a local measurement of the separation rate between a bubble and a low ballistic coefficient satellite would give an accurate measure of the local ambient density. For example, at 320-km altitude a 1-μm wall bubble separates from a $\beta = 0$ satellite with an acceleration of 0.07 m/s$^2$, in the direction opposite the velocity vector. This corresponds to a 100-m separation in just under 1 min.

Above roughly 600-km altitude, the radiant solar pressure becomes larger than the atmospheric drag. We have integrated a number of trajectories starting from circular orbits above 600 km including solar pressure. The orbits become roughly elliptical with the semiminor axis in the direction of the solar flux. The eccentricity increases rapidly and nearly linearly in time. For example, starting from 800 km, the maximum altitude initially increases by 6.7 km/orbit for a reflective 1-μm wall bubble.

### Atomic Oxygen

The major constituent of the ambient atmosphere in low Earth orbit is atomic oxygen. The total reactive energy available to an oxygen atom at orbital velocity is on the order of 10 eV. This large reactive energy can cause chemical changes in a surface. It has also been found to cause ablation of exposed surfaces. Since the proposed structures are so thin, they are very susceptible to disintegration in a short time by atomic oxygen ablation.

The time taken for a wall of thickness $\delta$ to entirely disintegrate is

$$\tau_d \sim \frac{\delta}{K(n\mathrm{v})} \tag{35}$$

where $(n\mathrm{v})$ is the atomic oxygen current density. The ablation rate $K$ is given by

$$K = \frac{\epsilon_{\mathrm{eff}} \mathrm{M}}{\rho_w N_A} \tag{36}$$

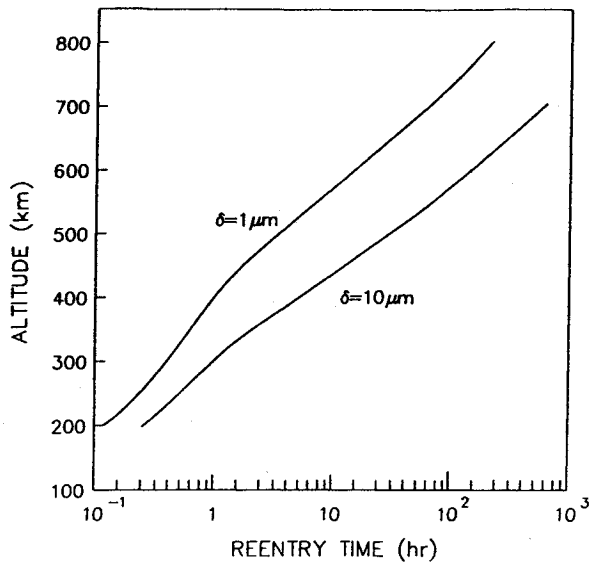


**Fig. 8 Orbital lifetime (to reach 150 km) as a function of altitude for a spherical bubble of different wall thicknesses.**

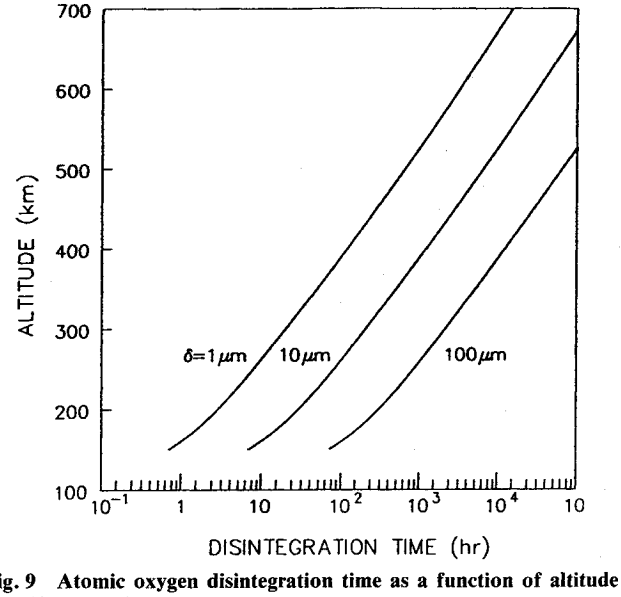


**Fig. 9 Atomic oxygen disintegration time as a function of altitude for different thicknesses.**

where $\epsilon_{\mathrm{eff}}$ is the efficiency of removing a molecule from the surface per incident atom. The ablation rate has been measured for a number of materials in low Earth orbit. For organic films similar to what might be used to form a bubble $K \sim 3 \times 10^{-24}$ cm$^3$/atom,[11] corresponding to an $\epsilon_{\mathrm{eff}}$ of about $10^{-4}$. The disintegration time for this $K$ and the atomic oxygen density of Ref. 9 is plotted in Fig. 9 for three different wall thicknesses. The lifetimes are measured in tens of hours at Shuttle altitude. This may eliminate most long duration applications of unprotected bubbles and thin films in low Earth orbit, but very short duration applications may make use of this limited lifetime. For example, given $K$, the time taken for a thin film of known thickness to disintegrate gives a measure of the atomic oxygen density. The film thickness could be measured by optical interference techniques. A more extensive treatment of the ablation problem in low Earth orbit is given elsewhere.[12]

## Conclusions

This study has identified and quantified the relevant effects of the Earth orbit environment on large diameter thin-wall

bubbles and films. These effects are all relevant to the use of gossamer structures in low Earth orbit. The principal results of this study are as follows.

1) Because the thin-wall bubble has an extremely low thermal mass, it is very efficiently coupled to the thermal environment and associated satellite. The thermal time constant is on the order of seconds. Very large temperature differences across the bubble ($\sim 100$ K) and temperature swings at the terminator ($\sim 100$ K) can be expected. This can lead to thermocapillary flow in a liquid wall, with a pressure gradient up to the order of the terrestrial hydrostatic gradient. The combination of large temperature differences and pressure gradients could deform or rupture a bubble or thin film. On the other hand, the strong thermal coupling to the environment makes the bubble a potentially useful tool in controlling spacecraft temperatures.

2) The low ambient pressure leads to very long mechanical damping times (hours) for a liquid wall bubble or thin film. The amplification of disturbances at the resonant frequency is also extremely large and could potentially make the structures unusable. A finite liquid vapor pressure also presents severe problems for forming a film or bubble. It may be necessary to keep the bubble open to the ambient pressure or an even lower pressure.

3) The ram pressure due to the orbital velocity through the ambient atmosphere can have a significant effect since it is on the order of the surface tension pressure for a curved liquid film. Deformations can occur, and the net ram force can even dislodge a liquid bubble from its associated satellite. This defines a maximum usable size for liquid wall bubble. Because of the enormous ballastic coefficient for a free bubble, its orbital lifetime is very short. This suggests tracking the bubble trajectory in order to measure the ambient density.

4) The ablation by atmospheric atomic oxygen is also significant for a thin film. This process would lead to a relatively short lifetime for unprotected films.

The gossamer nature of thin films and bubbles in Earth orbit makes them susceptible to the environmental effects listed above. Some of these suggest novel applications such as thermal radiators and probes of the ambient density. Others, such as low vacuum and atomic oxygen ablation, need to be considered in the design and use of these gossamer structures.

## Appendix: Damping in a Liquid Wall Bubble

We will consider the damping of spherically symmetric disturbances of a liquid wall bubble. Damping within the gas is neglected, and the bubble wall is assumed to be a Newtonian liquid with absolute viscosity $\eta$. The viscous force per unit volume is given by $-\eta \nabla^2 \boldsymbol{u}$, where $\boldsymbol{u}$ is the velocity field in the wall. The velocity in the wall can be calculated by assuming the liquid is incompressible. The positions of the inner and outer surfaces of the wall are

$$r_1 = r_0 + \xi \tag{A1a}$$

$$r_2 = r_0 + \delta + \xi \tag{A1b}$$

where $\delta$ is the wall thickess and $\xi$ the displacement from equilibrium. The velocity of the inner surface is simply

$$u(r_1) = \dot{\xi} \tag{A2a}$$

and, assuming the liquid is incompressible, the velocity of the outer surface, up to order $\xi/r_0$ and $\delta/r_0$, is

$$u(r_2) = [1 - (2\delta/r_0)]\dot{\xi} \tag{A2b}$$

The velocity in the wall is entirely radial and to first approximation a linear function of $r$. Given Eqs. (A2), therefore,

$$u(r) = [3 - (2r/r_1)]\dot{\xi} \qquad r_1 < r < r_2 \tag{A3}$$

The viscous force per unit volume is therefore

$$\frac{F_v}{4\pi^2\delta} = -\eta\left(\frac{6}{r_0^2}\right)\dot{\xi} \tag{A4}$$

The acceleration due to $F_v$ is

$$a_v = -(6\nu/r_0^2)\dot{\xi} \tag{A5a}$$

or

$$a_v = -2\gamma\dot{\xi} \tag{A5b}$$

with

$$\gamma = 3\nu/r_0^2 \tag{A6}$$

where $\gamma$ is the inverse decay time for spherical disturbances.

## Acknowledgments

This work was supported by Morton Thiokol, Inc., under Research Project 0288, and in part by the National Space Club through the Robert H. Goddard Fellowship. I would like to thank R. Gilbert Moore, L. Rex Megill, and Jan J. Sojka for many useful discussions about the results presented here.

## References

[1]Moore, R. G., "Bubble Structures for Gossamer Spacecraft," Conference on Gossamer Spacecraft, California Inst. of Technology, Pasadena, CA, Dec. 1979.

[2]Siegel, R., and Howell, J. R., *Thermal Radiation Heat Transfer,* McGraw-Hill, New York, 1972, Chap. 7.

[3]Davis, S. H., "Thermocapillary Instabilities," *Annual Review of Fluid Mechanics,* Vol. 19, 1987, pp. 403–435.

[4]Isenberg, C., *The Science of Soap Films and Soap Bubbles,* Tieto LTD., Avon, England, UK, 1978, Chap. 2.

[5]Picket, J. S., Murphy, G. B., Kurth, W. S., Goetz, C. K., and Shawhan, S. D., "Effects of Chemical Releases by the STS-3 Orbiter on the Ionosphere," *Journal of Geophysical Research,* Vol. 90, 1985, pp. 3487–3497.

[6]Kittel, C., and Kroemer, H., *Thermal Physics,* Freeman, San Francisco, 1980, Chap. 10.

[7]Davies, J. T., and Rideal, E. K., *Interfacial Phenomena,* Academic, New York, 1961, Chap. 5.

[8]Bickerman, J. J., *Physical Surfaces,* Academic, New York, 1970, Chap. 1.

[9]Cantor, A. J., Minzner, R. A., and Quiroz, R. S. (eds.), *U. S. Standard Atmosphere 1976,* U. S. Government Printing Office, Washington, DC, 1976, Pt. 4.

[10]Reiss, K., and O'Neil, J., "Tracking the GLOMR Satellite," 1986 Get Away Special Experimenter's Symposium, NASA CP 2438, Oct. 1986, pp. 1–8.

[11]Leger, L. J., and Visentine, J. T., "Low Earth Orbit Atomic Oxygen Effects on Surfaces," AIAA Paper 84-0548, Jan. 1984.

[12]Laher, R., "Ablation of Materials in the Low Earth Orbital Environment," Ph.D. Thesis, Utah State Univ., Logan, UT, 1987.

David H. Allen
*Associate Editor*